Optical Materials 150 (2024) 115232

Contents lists available at ScienceDirect

Optical Materials

journal homepage: www.elsevier.com/locate/optmat

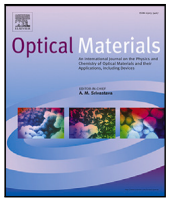

Research Article

# Optical transmission modulation and spectral properties of self-organized nematic domains

Alexander M. Parshin [a,b,*], Victor Ya. Zyryanov [a], Vasily F. Shabanov [a]

[a] Kirensky Institute of Physics, Federal Research Center KSC SB RAS, 50/38 Akademgorodok, Krasnoyarsk, 330036, Krasnoyarsk region, Russia
[b] Siberian Federal University,, 79 Svobodny Pr., Krasnoyarsk, 660041, Krasnoyarsk region, Russia

ARTICLE INFO

*Keywords:*
Nematic domains
Magnetic field
Electric field
Light modulation
Transmission spectrum

ABSTRACT

The modulation and spectral characteristics of self-organized ensembles of nematic domains with the disclination lines non-aligned and aligned in a magnetic field have been studied using an electric field. The obtained experimental voltage dependences of the light transmission agree well with the dependences calculated using the model considerations. These dependences have been compared with the electro-optical characteristics of a homogeneous planar nematic layer. The amplitude component of the optical transmission determined by light scattering and the oscillating component caused by the phase modulation have been examined. The effect of the spectral dispersion of transmission on the electro-optical characteristics of domain ensembles has been evaluated.

## 1. Introduction

Currently, the light modulation caused by nematic liquid crystal (LC) layers is being intensively studied and used in engineering devices [1–6]. The phase modulation manifests itself in the optical response of a homogeneous planar nematic layer (HPNL) to external magnetic field $H$ or electric field $E$. In the conventional $S$-effect geometry, an LC layer is localized in a cell between two transparent plane-parallel plates processed to form an HPNL and represents a linear wave plate [2]. When light falls onto an LC layer, two orthogonally polarized ordinary ($o$) and extraordinary ($e$) waves with respective refractive indices $n_e$ and $n_o$ arise. In the optical scheme, a polarizer and analyzer are used before and after the cell, the polarization directions of which are set at angles $\phi_1$ and $\phi_2$ to the director. Under the action of an external field, the LC director deviates by angle $\theta$ in the plane perpendicular to the cell surface and the index $n_e$ approaches the index $n_o$, which remains invariable. At $\phi_1 = \phi_2 = 0$, the phase modulation occurs. In the frequently used case $\phi_1 = \phi_2 = \pi/4$, the $o$- and $e$-waves projected onto one plane at the analyzer output interfere upon variation in $\theta$. The interference is caused by the phase difference between the waves and leads to the light transmission modulation [1]. By changing voltage $U$ through adding it with bias $U_b$ for fast switching between the transmission extrema, one can intensify the light modulation effects in the $S$-effect and use them in the birefringence control and monitoring systems $\Delta n = n_e - n_o$ with the help of an external field. The reorientation of the LC director to $U_b$ makes it possible to optimize the reorienting voltage amplitudes, switching times, and other parameters with a significant change in phase difference $\delta$, e.g., by $\pi$ [1,3].

The transmission modulation caused by the light phase modulation upon variation in the birefringence under the action of an external field can also be observed in the $B$-effect in LC cells with a homeotropic alignment of the director and in hybrid ordered nematics [3,7]. In the latter case, the LC layer has a homeotropic-planar molecular alignment and is located between two crossed polarizers. As shown in Ref. [7], the oscillating dependence of the light transmission on the applied electrical voltage exhibits a noticeable spectral shift, which can be used to create multicolor LC displays. The light modulation of various types [2,8] are manifested in twist cells, in which plane-parallel aligning plates are twisted by angle $\varphi$ relative to the perpendicular axis and a polarizer and analyzer are mounted at angles $\phi_1$ and $\phi_2$ relative to the nematic director. At $\varphi = \pi/2$ and $\phi_1 = \phi_2 = \pi/4$, only the phase modulation occurs, while at $\phi_1 = \pi/2$, $\phi_2 = \varphi + \pi/2$, there is only the amplitude modulation; at other angular ratios, the complex modulation of light is implemented. In addition, the second-order modulation effects [9] can be detected in twisted nematics, which arise even without an analyzer in the light path.

The complex modulation of light, in which, along with the interference oscillations, there are the amplitude changes in the transmission, manifests itself in the optical response of inhomogeneously aligned nematics to an external field. In particular, in LC droplets encapsulated in polymer matrices, the interference effects lead to the light transmission

* Corresponding author at: Kirensky Institute of Physics, Federal Research Center KSC SB RAS, 50/38 Akademgorodok, Krasnoyarsk, 330036, Krasnoyarsk region, Russia.
*E-mail address:* parshin@iph.krasn.ru (A.M. Parshin).

https://doi.org/10.1016/j.optmat.2024.115232
Received 21 October 2023; Received in revised form 26 February 2024; Accepted 13 March 2024
Available online 19 March 2024

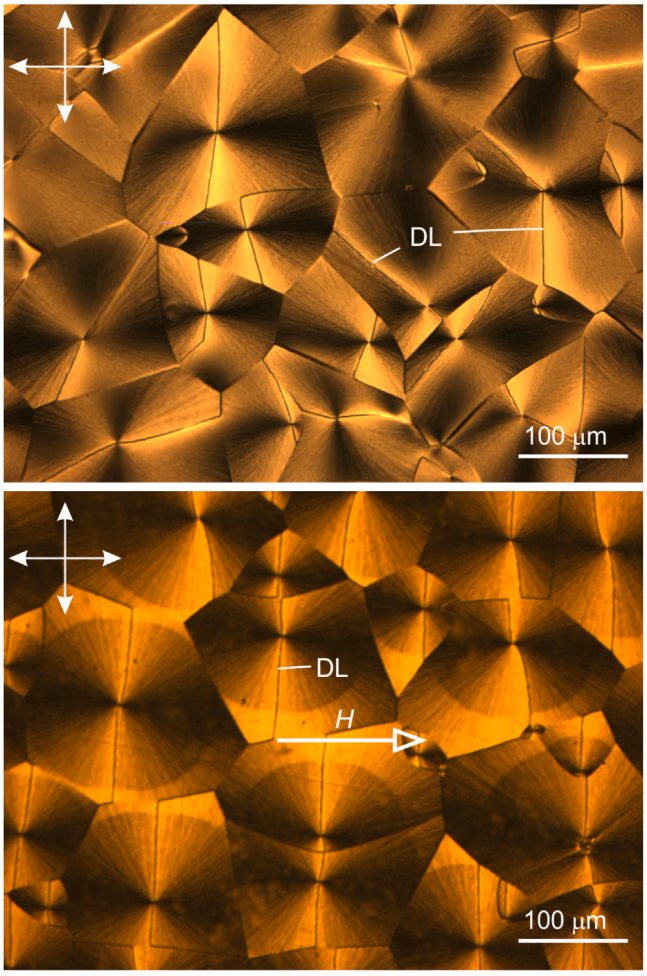


**Fig. 1.** The SEND texture microphotographs taken in crossed polarizers using a polarizing microscope with DLs (a) non-aligned and (b) aligned in magnetic field $H$. The SEND was formed during growth of 5CB domains on the polymer film obtained from the PC solution in dichloromethane.

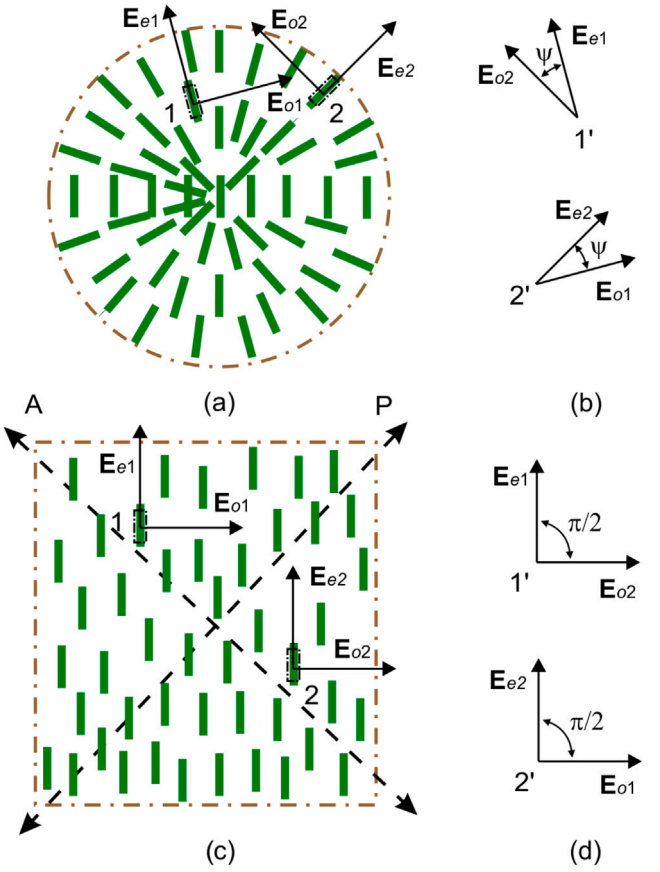


**Fig. 2.** Schematic of dividing a light wave into *o*- and *e*-components (Ee1, Eo1, Ee2, and Eo2) $\mathbf{E}_{e1}$, $\mathbf{E}_{o1}$, $\mathbf{E}_{e2}$, and $\mathbf{E}_{o2}$ in sections 1 and 2: (a) SEND, (b) HPNLs, and their superposition at photodetector points 1′ and 2′.

modulation in the optical scheme containing only a polarizer [10,11]. In such structures, the light scattering and structural parameters of droplets play an important role in the modulation processes. Similar effects are more pronounced in the dependences of the optical transmission of nematics on an electric field applied to the non-aligned LC layers [12–15]. The layers are domains of irregular shape 3–10 μm in size with a random director field distribution over angles $\phi$ and $\theta$. Recently, we have disclosed and explored self-organizing self-organized ensembles of nematic domains (SEND) that appear in LC 5CB on the polycarbonate (PC) film [16–20]. Domains 50–200 μm in size have a radial configuration with the disclination lines (DLs) extended into the bulk of an LC layer to structural coherence length $\xi$. The interference effects are investigate using electric and magnetic fields.

In this work, we study the modulation and spectral characteristics of the SEND in an electric field. The modulation of the light transmission through the SEND with non-aligned DLs is evaluated by calculation method and with DLs aligned magnetically is compared with the modulation of the transmission of a HPNL.

## 2. Model considerations of the light propagation through LC layers

In Fig. 1 the texture of the SEND in 5CB on the PC film with (a) the non-aligned and (b) magnetic-field-aligned DLs is shown. We consider the light transmission through an LC layer within the model developed by us earlier [19,20], in which an LC layer is presented by a set of crystal plates with an average size corresponding to the scale of equilibrium fluctuations of the order parameter [21]. The optical axis of each plate coincides with the LC director: it is directed along the major molecule axes (Fig. 2). The light wave falling onto a SEND perpendicular to the PC film (Fig. 1a) is divided into the ordinary ($o$) and extraordinary ($e$) components with respective refractive indices $n_o$ and $n_e$. At a large distance from the tested structure, the $\mathbf{E}_{e1}$, $\mathbf{E}_{o1}$, $\mathbf{E}_{e2}$, and $\mathbf{E}_{o2}$ components originating from excited plates 1 and 2 deviated due to the small-angle scattering are added in pairs at angle $\psi$ at photodetector points 1' and 2', as shown in Fig. 2. This superposition of $o$- and $e$-waves is realized due to the presence of a uniaxial phase in the nematic, in the layer of which the effective refractive index $n_{eff}$ is considered independent of the director field distribution over angles $\phi$ in any cross-section normal to the light beam [1]. Under the influence of an external field, $n_{eff}$ approaches $n_o$, and the phase difference $\delta$ between the $o$- and $e$-components changes when the LC director is rotated by an angle $\theta$ in the plane perpendicular to the PC film [20]. In this case, the angle $\psi$ in each SEND domain decreases in inverse proportion to the distance from the PC film, on which the radial configuration of the nematic director field is formed, to a uniform planar orientation at the coherence length $\xi$ [18]. This distance is determined by the electrical coherence length $\xi_E$, which increases in the same direction [20]. Therefore, the amplitude of the modulation of light passing through the LC layer does not depend on the distribution of the director field, but is determined by the effects of scattering on SEND inhomogeneities. The superposition of the waves causes their interference and transmission modulation, which does not require the

use of polarizers [19]. At the same time, in the HPNL (Fig. 2c), the angle $\psi$ between the vector pairs $\mathbf{E}_{e1}$, $\mathbf{E}_{o2}$ and $\mathbf{E}_{o1}$, $\mathbf{E}_{e2}$ is always right, so the *o*- and *e*-waves do not interfere. Therefore, to observe the interference, it is necessary to use polarizer P and analyzer A in the optical circuit (Fig. 2c). The projections of the o and e components onto the P and A vibration directions are brought in one plane, the waves interfere, and the optical transmission is modulated upon variation in $\delta$.

Using the standard procedure for minimizing the free energy of a SEND affected by electric field $E$, in Refs. [18,20] we obtained the equation for light intensity $I$, which, taking into account incident light intensity $I_0$, is presented as the transmission

$$T = \frac{1}{2}[1 + k\exp(-\sigma z)\cos\delta]. \quad (1)$$

This equation contains the exponential factor responsible for light scattering [20] and the cosine factor describing the oscillating nature of the change in intensity [22], in which $\sigma$ is the scattering cross section and $k$ is the structural coefficient. Such a generalized form of the equation makes it possible to better analyze the relationship between the amplitude and phase characteristics of light transmission by both the SEND (Fig. 2a) and HPNL (Fig. 2c). In the first case, we have $\sigma > 0$, $k = 2/\pi$ [20] and, in the second case, $\sigma = 0$, $k = -1$ [1]. The equation for the phase difference of the *o*- and *e*-waves passing through the SEND only will be used, which we write as [20]

$$\delta = \frac{2\pi n_0}{\lambda\left(A^2/\xi^2 + 1/\xi_E^2\right)} \times \int_0^{\pi/2} \left[\frac{n_e}{\left(n_e^2\cos^2\theta + n_o^2\sin^2\theta\right)^{1/2}} - 1\right]\frac{1}{\sin\theta}d\theta, \quad (2)$$

where $\lambda$ is the wavelength, $A = [(\pi^3/12 - \pi^2/4 + 1)/2\pi\ln(l/b)]^{1/2}$ [18], $l$ and $b$ are the DL length and width in a domain, $l = 2r$, $r$ is the domain radius, $\xi$ and $\xi_E = (1/E)(4\pi K/\Delta\epsilon)^{1/2}$ [17] are the structural and electrical coherence lengths, $K$ is the average modulus of elasticity, and $\Delta\epsilon$ is the dielectric anisotropy of an LC.

## 3. Experimental

Cells with plane-parallel glass plates coated with an indium tin oxide (ITO) conducting layer were used in the experiment. When fabricating a cell with the SEND in a centrifuge, a polymer film was deposited onto one plate from a 2% solution of PC in dichloromethane. The other plate was not processed to any orientation, but was only washed with boiling acetone and hexane. The plates were stacked with each other through Teflon spacers specifying a gap of 35 μm and glued together. The gap of cell complied with the requirement that the thickness of LC layer should be significantly greater than the coherence length $\xi \approx 17$ μm [18], at which a modulation appears. The cell was filled with the nematic 5CB (4-n-pentyl-4'-cyanobiphenyl) in the mesophase. Within 20 min, LC domains grew on the PC film and a domain structure [16] with a typical SEND texture formed in the cell (Fig. 1a). To obtain a structure with the texture presented in Fig. 1b, the filled cell was placed between the N–S poles of an electromagnet (Fig. 3) with a magnetic field of $H = 25$ kOe aligning the DLs preferable perpendicular to $H$. To form the cell with the HPNL, two glass plates were coated with a polymer film obtained from the 4% polyvinyl alcohol (PVA) solution. A microrelief was created on the plates by unidirectional rubbing with a velveteen cloth. The plates were stacked through Teflon spacers specifying a gap of 13.8 μm with the coinciding rubbing directions and glued together. The gap was adjusted so that the thickness of the LC layer $d$ can be comparable with the coherent length $\xi'$ in order to be able to use the cell as a reference when the modulation characteristics of SEND with the DLs aligned in a magnetic field will be studied. In such cells, the values of $\xi'$ are always slightly lower than the values of $\xi$ in SEND formed in the absence of a magnetic field, and in this case, we can assume $d \approx \xi'$. The cell was filled with 5CB in the isotropic phase to avoid inhomogeneities in the LC layer. The size of the cell gaps both for the SEND and the HPNL is determined using the

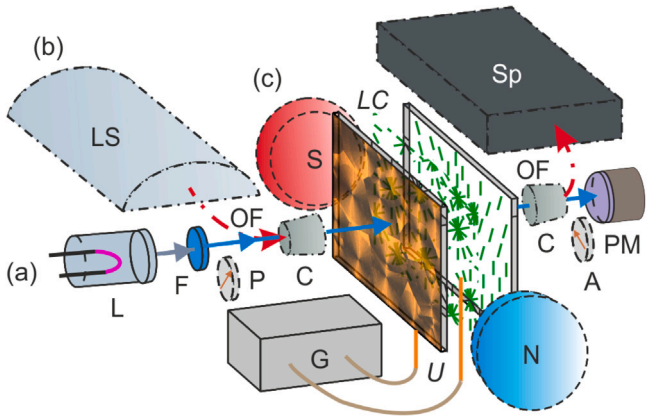


**Fig. 3.** Scheme of the setup (a) for obtaining the electro-optical characteristics (halogen lamp L, filter F, polarizer and analyzer P and A, photomultiplier PM, and generator G), (b) for recording the spectral characteristics (light source LS, optical fibers OF, collimators C, and spectrometer Sp), and (c) electromagnet for forming the SEND with aligned DLs.

interference extremes of light waves reflected from upper and lower cell surfaces. All processes occurred at a temperature of 23 °C.

The electro-optical characteristics of the cells were obtained on a setup presented in Fig. 3. Light from a halogen lamp L was pass through filter F and fell on the cell with LC perpendicular to the plates. The transmission $T$ was recorded using a photomultiplier PM. A slowly increasing voltage $U$ was applied to the cell from a generator G with a frequency of 1 kHz and the $T(U)$ dependence was plotted using a computer program. We did not observe burning of cells up to a voltage of 80 V. Apparently, this is prevented by PC and PVA polymer coatings on the cell substrates. When the cells with the SEND were used, polarizers were not introduced into the optical path. The cross polarizer P and analyzer A were installed on the light path at an angle $\pi/4$ to the director (Fig. 1c) before and after the cells with the HPNL. To obtain the $T(\lambda)$ spectral dependences, an Ocean Optics HR4000 spectrometer Sp was used, which received radiation from a light source LS with halogen and deuterium lamps via optical fibers OF through collimators C.

## 4. Results and discussion

The experimental (1) and calculated (2) $T(U)$ dependences are presented in Fig. 4. It can be seen that they agree well. The calculated dependence was obtained from Eqs. (1) and (2) at $\lambda = 663$ nm, $k = 2/\pi$, $\sigma = \xi = 16.7$ μm, $l = 2r = 96$ μm, $A = 0.332$, $K = 6.21$ pN, $\Delta\chi = 1 \cdot 10^{-7}$, $\Delta\epsilon = 13.8$ [23], $n_o = 1.5271$, $n_e = 1.7103$ [24], $z = \xi_E$, and $U = 1.5 - 80$ V. The literature data on the 5CB parameters at a temperature of 23 °C were used. The dependences reflect the modulation of the transmission of the light flow consisting of the amplitude and oscillating components. The amplitude component is determined by the light scattering and described by the exponential factor in Eq. (2). Indeed, the envelopes of the first three maxima and four minima on the logarithmic scale are straights. The last maximum, however, does not meet this regularity and is located far from the envelope. This can be easily explained by the fact that, with an increase in field $E$, the electrical coherence length $\xi_E$ tends to zero, the exponential factor in Eq. (1) vanishes, and the transmission extremum $T$ on the plot approaches its maximum position $T_H$ corresponding to the homogeneous homeotropic orientation of the nematic. This position is slightly lower than the limit value $T_m = 1$ due to the stationary scattering [1] on inhomogeneities of the SEND, which is independent of the change in angle $\theta$ under the action of an external field. The oscillating component is caused by the phase modulation of light and corresponds to the second factor in Eq. (1). The phase difference of the

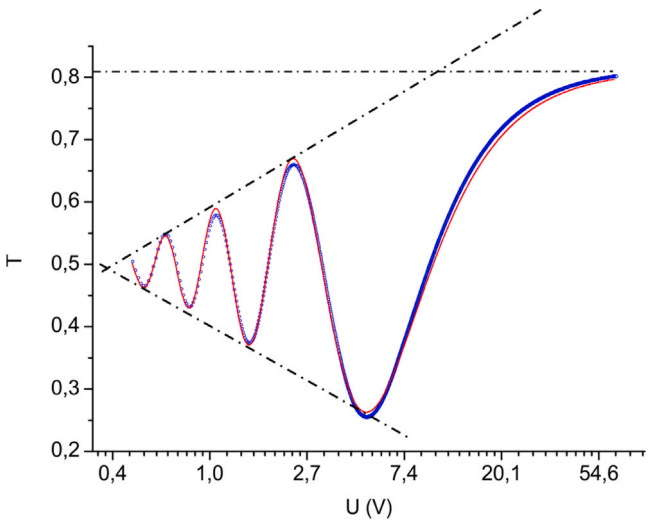


**Fig. 4.** Experimental (blue circles) and calculated (red solid curve) voltage dependences of transmission $T$ of light passed through the SEND.

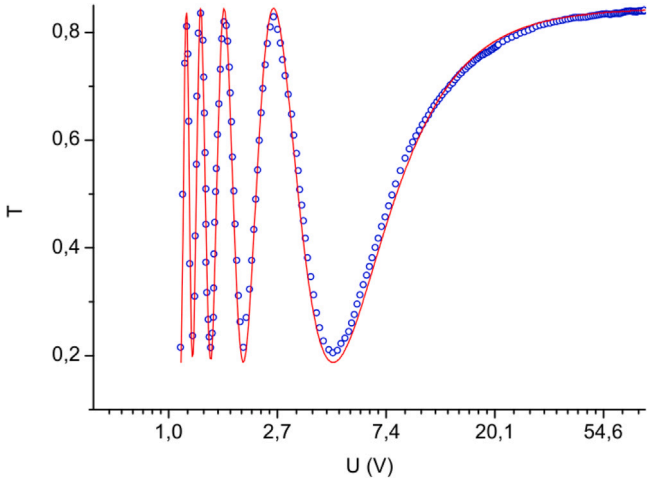


**Fig. 5.** Experimental (blue circles) and (red solid curve) calculated voltage dependences of transmission $T$ of light passed through the SEND with the DLs aligned in a magnetic field.

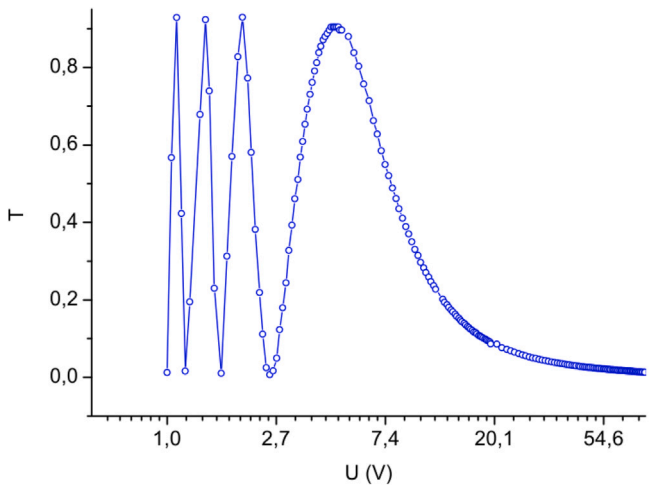


**Fig. 6.** Experimental data (circles and a line connecting them) for voltage dependence of transmission $T$ of light passed through the HPNL.

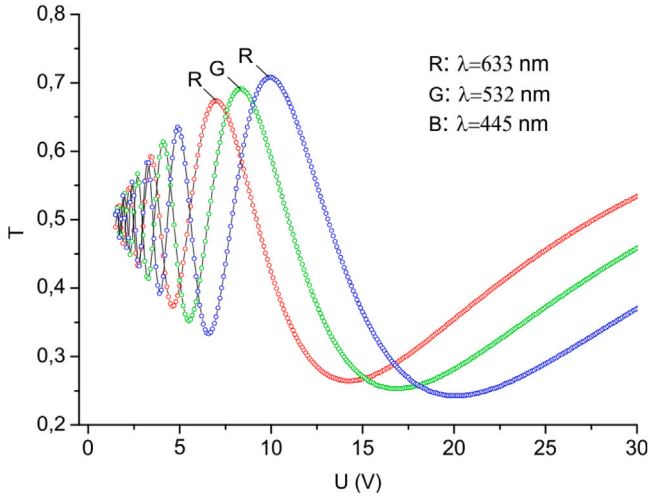


**Fig. 7.** Experimental data (circles and a line connecting them) for voltage dependences of transmission $T$ of light passed through the SEND at different light wavelengths $\lambda$.

*o*- and *e*-waves occur at the structural coherence length $\xi$ within which the radial structure is preserved [18].

The light scattering weakens significantly when the DLs in the SEND are ordered in a magnetic field, since the main contribution to the light beam deflection comes from interdomain inhomogeneities caused by the misorientation of the DLs [19]. The $T(U)$ dependence for the SEND with the aligned DLs is presented in Fig. 5. It can be seen that the transmission value corresponding to the last maximum, as for the SEND with the non-aligned DLs, remains below $T_H$; however, other maxima are pulled up to it. The positions of the minima also align. The dependence becomes similar to the $T(U)$ dependence for the HPNL (Fig. 6) obtained in the optical circuit with crossed polarizers (Fig. 3). The latter dependence is sinusoidal, since it originates from zero $T$ and $U$ values and the last extremum becomes the minimum. In fact, the $T(U)$ dependence for the SEND with the aligned DLs corresponds to the $T(U)$ dependence with the phase modulation for the HPNL, but is shifted from it in phase by $\pi/2$. This behavior of $T$ follows from Eq. (1), since if we allow $k = 1$ for the SEND, then, in the absence of scattering depending on $\theta$, the light transmission will be $T = \cos^2 \delta/2$ and, for the SEND, at $k = -1$, will be determined as $T = \sin^2 \delta/2$.

The electro-optical $T(U)$ characteristics, as follows analytically from Eqs. (1) and (2), should depend on wavelength $\lambda$. In Fig. 7 is shows the $T(U)$ dependences for the SEND at different $\lambda$ values corresponding to the primary colors red (R), green (G), and blue (B) of the visible range, which were obtained without polarizers using filters in the electro-optical scheme (Fig. 3). In the plot, one can see the splitting of the transmi maxima in the R, G, and B curves. At the same time, the curves have different oscillation periods and, therefore, their superposition is voltage-dependent.

Using bias voltage $U_b$, one can reconstruct the spectral characteristics. In Fig. 8, the transmission spectra at $U_b$ = 3.9, 8.3, and 9.9 V are shown, which correspond to the $U$ values at the maxima of the R, G, and B curves in Fig. 7. All the $U(\lambda)$ dependences have maxima in the corresponding parts of the spectrum, but the R curve has a minimum, which is close to the maximum of the B curve in the blue portion of the spectrum. The superposition of the shifted components yields a transmission value close to the initial level. In other words, setting the $U_b$ values at the maxima of the R, G, and B curves, the adjacent components can be shifted by $\pi$, which ensures their fast switching.

The $T(U)$ dependence for the SEND at all $\lambda$ values in the visible range is shown in Fig. 9. The 3D plot clearly shows the degree of effect of the optical transmission dispersion on the electro-optical characteristics of the SEND when using the non-monochromatic light.

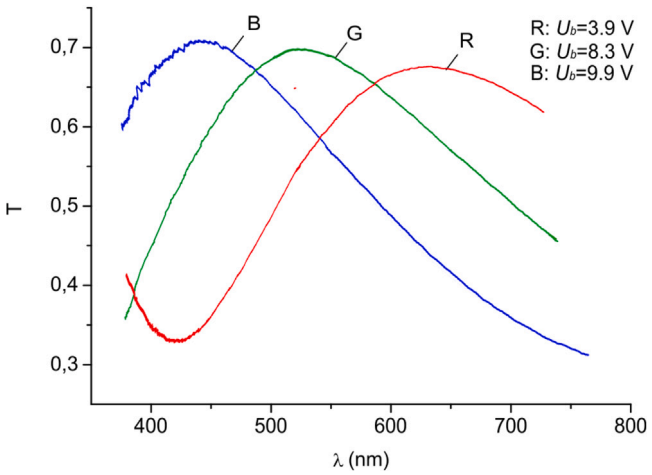


**Fig. 8.** Transmission spectra for the SEND at bias voltages $U_b$ of 3.9, 8.3, and 9.9 V.

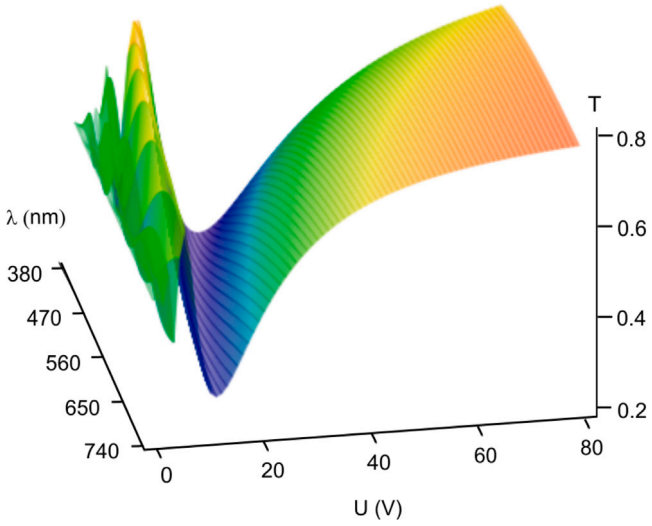


**Fig. 9.** Calculated spectral and voltage dependences of transmission $T$ of light passed through the SEND.

## 5. Conclusion

The transmission modulation and spectral characteristics of the radial-planar SEND were studied using an electric field. The structures were formed in plane-parallel cells in the 5CB nematic layers during the growth on a PC film. The SEND with the DLs non-aligned and aligned magnetically were investigated. The propagation of light through the LC layer was examined within the model developed by us previously using the equations for the optical transmission and phase difference between the *o*- and *e*-waves. The transmission equation contains the exponential factor responsible for the light scattering and the cosine component describing the oscillating nature of the intensity variation. Using the literature data on 5CB, the calculated dependences of transmission $T$ on voltage $U$ for the SEND were obtained. The experimental electro-optical characteristics of the SEND in the form of the $T(U)$ dependences were obtained on a setup consisting of a halogen lamp, a filter, and a photomultiplier. The experimental dependences were found to be in good agreement with the calculated ones.

The modulation characteristics of the SEND and HPNL were compared. The $T(U)$ dependences for the HPNL were recorded with two crossed polarizers in the electro-optical scheme. It was shown that, in the SEND with the DLs aligned in a magnetic field, the scattering component decreases sharply from the optical transmission and the $T(U)$ curve approaches the same curve obtained for the HPNL. At the same time, the light propagation processes in the investigated structures are qualitatively different. In the SEND, the phase difference of the *o*- and *e*-waves occur at the structural coherence length $\xi$ within which the radial structure is preserved. The superposition of the *o*- and *e*-waves leads to their interference and transmission modulation, the manifestation of which does not require the use of polarizers. It should be emphasized that to observe the interference and transmission modulation in the HPNL, one should obtain the projections of the *o*- and *e*-waves and bring them in one plane on a detector using only two-polarizer optical scheme.

The spectral dispersion of the optical transmission was examined. In the $T(U)$ dependences obtained for monochromatic light, the splitting of the transmission maxima of the R, G, and B curves was revealed. The curves have different oscillation periods; therefore, the positions of their extrema depend on the voltage. The use of bias voltage $U_b$ allows one to shift the spectral characteristics. For example, fixing the $U_b$ values at the maxima of the R, G, or B curves, these curve's components can be shifted by $\pi$, ensuring their fast switching. The degree of impact of the optical transmission dispersion on the electro-optical characteristics of the SEND when using the non-monochromatic light is shown in the 3D plot.

## CRediT authorship contribution statement

**Alexander M. Parshin:** Conceptualization, Data curation, Formal analysis, Investigation, Software, Visualization, Writing – original draft. **Victor Ya. Zyryanov:** Conceptualization, Methodology, Software, Validation, Visualization, Writing – review & editing. **Vasily F. Shabanov:** Conceptualization, Project administration, Validation, Visualization, Writing – review & editing.

## Declaration of competing interest

The authors declare that they have no known competing financial interests or personal relationships that could have appeared to influence the work reported in this paper.

## Data availability

No data was used for the research described in the article.

## References

[1] L.M. Blinov, Structure and Properties of Liquid Crystals, Springer, London, 2011, http://dx.doi.org/10.1007/978-90-481-8829-1.

[2] A. Forbes, Laser Beam Propagation, Taylor and Francis, New York, 2014, http://dx.doi.org/10.1201/b16548.

[3] D.A. Yakovlev, H.S. Kwok, Modelling and Optimization of LCD Optical Performance, Wiley and Sons, Chichester, 2015, http://dx.doi.org/10.1002/9781118706749.

[4] E. Perez-Cabre, M.S. Millan, Liquid crystal spatial light modulator with optimized phase modulation ranges to display multiorder diffractive elements, Appl. Sci. 9 (2019) 2592-1–2592-14, http://dx.doi.org/10.1007/s11837-013-0675-3.

[5] S.-W. Jang, W. Choi, S. Kim, J. Lee, S. Na, S. Ham, J. Park, H. Kang, B.-K. Ju, H. Kim, Complex spatial light modulation capability of a dual layer in-plane switching liquid crystal panel, Sci. Rep. 12 (2022) 8277-1–8277-14, http://dx.doi.org/10.1038/s41598-022-12292-4.

[6] M.L.N.M. Mohan, K. Pal, Liquid crystalline light modulation mechanism and shuttering applications, in: K. Pal, S. Thomas (Eds.), Functional Material Processing for Switchable Device Modulation, Elsevier, 2021, http://dx.doi.org/10.1016/C2020-0-01203-X.

[7] S. Matsumoto, M. Kawamoto, K. Mizunoya, Fiel-induced deformation of hybrid-aligned nematic liquid crystals: new multicolor liquid crystal display, J. Appl. Phys. 47 (1976) 3842–3845, http://dx.doi.org/10.1063/1.323245.

[8] E.G. van Putten, I.M. Vellekoop, A.P. Mosk, Spatial amplitude and phase modulation using commercial twisted nematic LCDs, Appl. Opt. 47 (2008) 2076–2081, http://dx.doi.org/10.1364/AO.47.002076.

[9] J.A. Davis, P. Tsai, D.M. Cottrell, T. Sonehara, J. Amako, Transmission variations in liquid crystals ligh modulators caused by interference and diffraction effects, Opt. Eng. 38 (1999) 1051–1057, http://dx.doi.org/10.1117/.1.602149.
[10] V.V. Presnyakov, V.Ya. Zyryanov, A.V. Shabanov, S.Ya. Vetrov, Mol. cryst. Fried-ericksz threshold in bipolar nematic droplets with rigidly fixed poles, Mol. Cryst. Liq. Cryst. 329 (1999) 27–34, http://dx.doi.org/10.1080/10587259908025922.
[11] A.V. Barannik, V.F. Shabanov, V.Ya. Zyryanov, V.I. Lapanik, V.S. Bezborodov, Interference and ion effects in the electro-optical response of PDNLC films, J. Soc. Inf. Disp. 13 (2005) 273–279, http://dx.doi.org/10.1889/1.1904926.
[12] N. Aryasova, A. Iljin, V. Reshetnyak, Yu. Reznikov, A. Glushchenko, J. West, Orientation of nematic liquid crystals on random anchoring surface, Mol. Cryst. Liq. Cryst. 375 (2002) 165–173, http://dx.doi.org/10.1080/10587250210593.
[13] O. Hotra, I. Lopatyanscyj, B. Yavorskyj, New electro-optical effect in liquid crystal for integrated optics elements, Proc. SPIE 5124 (2003) 112–114, http://dx.doi.org/10.1117/12.517065.
[14] D.D. Yakovlev, D.A. Yakovlev, Scattering patterns of orthogonally components for statistically rotationally invariant mosaic birefringent layers, Opt. Spectrosc. 126 (2019) 245–256, http://dx.doi.org/10.1134/s0030400x19030238.
[15] D.D. Yakovlev, M.M. Sherman, A.A. Murauski, D.A. Yakovlev, Features of light scattering on mosaic layers composed of structurally similar birefringent domains, J. Mod. Opt. 67 (2020) 111–125, http://dx.doi.org/10.1080/09500340.2019.1697833.
[16] A.M. Parshin, V.A. Gunyakov, V.Ya. Zyryanov, V.F. Shabanov, Int. j. mol. sci, domain structures in nematic liquid crystals on a polycarbonate surface, Int. J. Mol. Sci. 14 (2013) 16303–16320, http://dx.doi.org/10.3390/ijms140816303.
[17] A.M. Parshin, V.A. Gunyakov, V.Ya. Zyryanov, V.F. Shabanov, Electric and magnetic field-assisted orientational transitions in the ensembles of domains in a nematic liquid crystal on the polymer surface, Int. J. Mol. Sci. 15 (2014) 17838–17851, http://dx.doi.org/10.3390/ijms151017838.
[18] A.M. Parshin, V.Ya. Zyryanov, V.F. Shabanov, The director field distribution with the strongly pinned alignment in nematic structures at the polymer surface, Liq. Cryst. 42 (2015) 57–64, http://dx.doi.org/10.1080/02678292.2014.960904.
[19] A.M. Parshin, A.V. Barannik, V.Ya. Zyryanov, V.F. Shabanov, Interference of nonpolarized light inliquid crystal domains on a polycarbonate surface, J. Opt. Soc. Am. B 36 (2019) 1845–1849, http://dx.doi.org/10.1364/JOSAB.36.001845.
[20] A.M. Parshin, V.Ya. Zyryanov, V.F. Shabanov, Self-organized ensembles of nematic domains in magnetic and electric fields, Phys. Rev. E 106 (2022) 024703, http://dx.doi.org/10.1103/PhysRevE.106.024703.
[21] P.G. de Gennes, J. Prost, The Physics of Liquid Crystals, Clarendon Press, Oxford, 1993, http://dx.doi.org/10.1063/1.2808028.
[22] M. Born, E. Wolf, Principles of Optics, CUP, Cambridge, 1999, http://dx.doi.org/10.1016/S0030-3992(00)00061-X.
[23] M.J. Bradshaw, E.P. Raynes, J.D. Bunning, T.E. Faber, The Frank constants of some nematic liquid crystals, J. Phys. France 46 (1985) 1513–1520, http://dx.doi.org/10.1051/jphys:019850046090151300.
[24] J.D. Bunning, D.A. Crellin, T.F. Faber, The effect of molecular biaxiality on the bulk proper-ties of some nematic liquid crystals, Liq. Cryst. 1 (1986) 37–51, http://dx.doi.org/10.1080/02678298608086488.